# Explosion dynamics of rare-gas clusters in an intense laser field

Kenichi Ishikawa* and Thomas Blenski
*Service des Photons, Atomes et Molécules, Centre d'Etudes Nucleaires de Saclay, Commissariat à l'Energie Atomique, 91191 Gif-sur-Yvette Cedex, France*

(Received 26 April 2000; revised manuscript received 17 July 2000; published 15 November 2000)

We study the explosion dynamics of rare-gas clusters ($Ar_{55}$, $Ar_{147}$, $Xe_{55}$, and $Xe_{147}$) in an intense, femtosecond laser pulse via Monte Carlo classical particle-dynamics simulations. Our method includes tunnel and impact ionization as well as ion-electron recombination, and allows us to follow the motion of both ions and free electrons during laser-cluster interaction. Our simulation results show that ionization proceeds mainly through tunnel ionization by the combined fields from ions, electrons, and laser while the contribution of electron-impact ionization is secondary. The ions are ejected in a stepwise manner from outer shells and accelerated mainly through their mutual Coulomb repulsion. Taking a spatial laser intensity profile into account, we show that the Coulomb explosion scenario leads to the same charge dependence of ion energy, i.e., quadratic for lower charge states and linear for higher ones, as that observed in experiments with larger clusters. This indicates that Coulomb explosion may be a dominant cluster explosion mechanism even in the case of large clusters. We also find that the ion energy is higher in the direction parallel to laser polarization than in the direction perpendicular to it. When ions are emitted along the direction of laser polarization, their charge changes in phase with the laser field, and this leads to an efficient acceleration.

PACS number(s): 36.40.Vz, 07.05.Tp

## I. INTRODUCTION

Since the advent of high-intensity ($>10^{14}\,W/cm^2$), short-pulse ($<1$ ps) lasers, their interaction with rare-gas clusters has been extensively studied [1–13]. Although the global density of a cluster gas may be arbitrarily low, its high local density leads to strong absorption of laser energy. The experimental observation of highly charged ions [1,2], high-ion kinetic energy [3], high-electron temperature [4], and x-ray emission in the keV range [5] has revealed a surprisingly high energetic nature of the interaction.

Theoretical modeling of the intense laser pulse interaction with rare-gas clusters is a challenging subject involving the nonlinear, nonperturbative response of many ions and electrons. The laser-cluster interaction involves two processes, i.e., ionization and explosion. Several models have been developed on the ionization mechanism which leads to the production of unusually high charge states. In a coherent electron motion model by Boyer *et al.* [6], multiple ionization arises from impact by coherently moving electrons, behaving like a quasiparticle. Ditmire *et al.* [7,9] proposed a ''nanoplasma'' model, in which ions are ionized mainly through the impact of hot electrons heated by inverse bremsstrahlung. Rose-Petruck *et al.* [10] introduced an ''ionization ignition (II)'' model, where ionization is driven by the combined field of the laser, the other ions, and the electrons. The explosion dynamics, responsible for the high-ion energy, has been less exploited in the theoretical modeling. The nanoplasma model [7,9] suggests that the cluster expands in a hydrodynamic manner by the pressure of hot electrons confined inside the cluster by the space-charge effect. However, Last and Jortner [11–13] performed classical dynamics simulations, and showed that electrons are quickly removed even from large xenon clusters containing over 1000 atoms due to a quasiresonance energy enhancement, and, therefore, that the existence of the nanoplasma confined inside the cluster is questionable.

In the present study we investigate the explosion dynamics of rare-gas clusters irradiated by an ultrashort intense laser pulse using Monte Carlo classical particle-dynamics simulations. Classical particle-dynamics simulations have already been used to study laser-cluster interaction by several authors [9,10,13]. However, these authors mainly studied the ionization dynamics, and up to now, to our knowledge, there has been no detailed work on the dynamics of ions ejected from an exploding cluster, such as the dependence of their kinetic energy on their charge state or emission angle. Such dependence has been experimentally measured [2,8,14] in order to study the cluster explosion dynamics, and its simulational investigation is the main concern of the present study, though we also discuss the ionization mechanism briefly. We simulate the explosion of $Ar_{55}$, $Ar_{147}$, $Xe_{55}$, and $Xe_{147}$. This cluster size is larger than that in Ref. [9] and smaller than in Ref. [13]. In principle we can treat even larger clusters, but we limit the cluster size to the values given above in order to obtain sufficiently good statistics for the discussions in the present study.

The present paper is organized as follows. Section II summarizes our simulation method. Although we take an approach similar to those in Refs. [9] and [13], we include two important improvements over these previous methods: the use of real (singular) Coulomb potential from ions and the implementation of ion-electron recombination. It appears that the recombination plays an important role in the explanation of the angular dependence of ion energy in Sec. V. In Sec. III we discuss the importance of tunnel and electron-

*Present address: Laser Technology Laboratory, Institute of Physical and Chemical Research (RIKEN), 2-1 Hirosawa, Wako-shi, Saitama 351-0198, Japan. Email address: ishiken@postman.riken.go.jp

 

impact ionization in laser-cluster interaction. Our results indicate that the former is the dominant ionization mechanism and that the latter plays only a minor role. In Sec. IV we examine the charge dependence of ion energy. Experimental work by Lezius *et al.* [2] has shown that the dependence is quadratic in the case of $Ar_N$ ($N \approx 1.8\times 10^5$) while it is quadratic at lower charge states and linear at higher charge states in the case of $Xe_N$ ($N \approx 2.0\times 10^6$). In recent experiments with $Pb_N$ ($N \approx 300$), Viallon [14] has found a charge-energy relation similar to the case of $Xe_N$. In Refs. [2] and [14] the quadratic dependence was attributed to Coulomb explosion, and the linear one to hydrodynamic expansion. However, our simulation, in which the Coulomb explosion is shown to be a dominant mechanism, leads to a similar behavior. Thus we show that this charge-energy relation can be entirely explained on the basis of the Coulomb explosion mechanism if we take a spatial laser intensity profile into account properly. In Sec. V we study the dependence of ion energy on the emission angle with respect to the laser polarization. We find that the energy of ions is higher when they are emitted along the direction of laser polarization. This can be connected to the change of their charge state during an optical cycle and the resulting laser-induced acceleration. The conclusions are given in Sec. VI.

## II. SIMULATION METHOD

A basic idea of our simulation method is to treat ions and free electrons as classical point particles and to integrate the nonrelativistic equations of motion for them. Bound electrons do not appear explicitly. This idea is based on the fact that the essence of many phenomena involving an intense laser field, such as above-threshold ionization [15] and high-order harmonic generation [16], can be well described by treating the ejected electron as a classical particle without taking account of the response of bound electrons. The force acting on each particle is calculated as the sum of the contributions from all the other particles and the laser electric field. To account for the finite size of the electron cloud around each nucleus, the field from an ion of charge state $Q$ is modeled as a Coulomb one from an effective nuclear charge $Q_{\rm eff}(r)$ of the form,

$$Q_{\rm eff}(r)=\begin{cases} Z(1-r/r_a) & \text{for} \quad r<(Z-Q)r_a/Z, \\ Q & \text{for} \quad r\geqslant(Z-Q)r_a/Z, \end{cases} \tag{1}$$

with $Z$ being the atomic number and $r_a$ the ''atomic radius,'' calculated using self-consistent-field functions [17], which takes the value of 1.3 a.u. for Ar and 2.0 a.u. for Xe. We use atomic units throughout this paper unless otherwise stated. $Q_{\rm eff}(r)$ tends to the bare nuclear charge $Z$ as $r$ tends to zero. This potential is more suitable for the description of ion-electron interaction, which may lead to the confinement of electrons inside the cluster and inverse bremsstrahlung, than a soft Coulomb potential used by Ditmire [9]. The equation of motion of particles are integrated with the fifth order Cash-Karp Runge-Kutta method with adaptive step-size control [18]. In a situation where an electron happens to be very close to an ion, the use of a real Coulomb potential might lead to serious problems, i.e., very small time steps and numerical heating. To circumvent these problems, we resort to Kustaanheimo-Stiefel regularization [19–21] (also see the Appendix), widely used in astrophysical simulations. This is an efficient method to transform the equations of the relative two-body motion into a form that is well behaved for small separations.

In an intense laser field, the cluster atoms may be ionized by tunnel ionization (field ionization). We evaluate the probability of ionization per unit time $W_{\rm tun}$ from a state with orbital number $l$ of an ion with charge $Q$ via the following analytic formula [22,23]:

$$W_{\rm tun}=\sum_{m=-l}^{l}\frac{(l+|m|)!}{2^{|m|}|m|!(l-|m|)!}\left(\frac{2e}{n^*}\right)^{2n^*}\frac{I_p}{2\pi n^*} \times\left(\frac{2(2I_p)^{3/2}}{E}\right)^{2n^*-|m|-2}\exp\left(-\frac{2(2I_p)^{3/2}}{3E}\right), \tag{2}$$

where $I_p$ denotes the ionization potential, $E$ the total electric field seen by the ion, and $n^*$ the effective principal quantum number defined by

$$n^*=(Q+1)[2I_p]^{-1/2}. \tag{3}$$

If a random number $p\in[0,1]$ is smaller than the tunneling probability $W_{\rm tun}\Delta t$ during a time step $\Delta t$, the tunnel ionization occurs. Then a new electron is placed with zero velocity near the parent ion in the direction of the ionizing field in such a way that the total energy of the system is conserved. Depending on the positions of the ions and the other electrons, there happens to be situations where it is impossible to put a new electron into the simulated system, guaranteeing the energy conservation at the same time. In such cases, ionization is cancelled.

Free electrons may appear also through electron-impact ionization (collisional ionization). An electron-impact ionization takes place if the distance between an electron and an ion is decreasing and if the impact parameter $b$ and the electron-impact ionization cross section $\sigma_{\rm EII}$ satisfy the relation

$$4\pi r_0|r_0-b|<\sigma_{\rm EII}, \tag{4}$$

where $r_0$ is obtained from

$$U_{Q+1}(r_0)=I_p, \tag{5}$$

with $U_Q(r)$ being the potential of an ion with a charge of $Q$. We use such a value of the impact parameter $b$ that we would obtain by integrating back the trajectory of the ion and the electron to $t=-$infinity as if there were no other ions, electrons, or the laser fields. This value can be calculated analytically using the conservation of momentum and angular momentum. We calculate $\sigma_{\rm EII}$ using fitting formulas by Lennon *et al.* [24] for Ar and the Lotz formula [25],

$$\sigma_{\rm EII}=a\,q\,\frac{\ln(E_e/I_p)}{E_eI_p} \quad (E_e>I_p) \tag{6}$$

for Xe, where $a=4.5\times10^{-14}\,\mathrm{cm^2\,eV^2}$, $q$ is the number of electrons in the outer shell of the ion, and $E_e$ is the energy of the impact electron. In Eq. (6) we have taken into account only the dominant first term of the original Lotz formula [25]. Upon ionization a new electron is placed at the distance $r_0$ from the ion with the position and velocity chosen randomly with the condition that the total energy and momentum are conserved.

In the laser-cluster interaction free electrons may be recombined with ions. The main recombination mechanisms are radiative and three-body recombination. Since our simulation method does not include radiative processes, it is impossible to treat the former correctly. The treatment of the latter, though it is possible in principle, would be extremely complicated since we have to take into account the motion of all the ions and electrons. Instead, therefore, we propose a simple treatment of recombination as follows: a pair of an ion with a charge $Q$ and an electron is replaced by an ion with a charge $Q-1$ if the distance between them is decreasing, if there is no potential barrier between them, and if the following relation is satisfied:

$$\sum_j \left[Q_j/|\mathbf{X}-\mathbf{X}_j| - U_{Q_j}(|\mathbf{x}-\mathbf{X}_j|)\right] - \sum_i \left( U_Q(|\mathbf{X}-\mathbf{x}_i|) - U_{Q-1}(|\mathbf{X}-\mathbf{x}_i|) - \frac{1}{|\mathbf{x}-\mathbf{x}_i|}\right) - U_Q(|\mathbf{x}-\mathbf{X}|) + \mathbf{F}_L\cdot(\mathbf{x}-\mathbf{X}) + \frac{v^2}{2} < 0, \tag{7}$$

where $\mathbf{x}$ is the electron position, $\mathbf{X}$ the ion position, $\mathbf{F}_L$ the laser field, and $v$ the electron velocity. The first sum is taken over all the other ions $j$ of a position $\mathbf{X}_j$ and a charge $Q_j$, and the second sum over all the other electrons $i$ of a position $\mathbf{x}_i$. If there were no other ions or electrons than the ion-electron pair, the inequality Eq. (7) would be reduced to the following expression:

$$-U_Q(|\mathbf{x}-\mathbf{X}|) + \mathbf{F}_L\cdot(\mathbf{x}-\mathbf{X}) + \frac{v^2}{2} < 0, \tag{8}$$

which states that the total energy of the electron is negative. The first two terms of Eq. (7) are the correction due to the presence of the other ions and electrons. The inclusion of recombination has the following advantage. A problem which may be encountered in classical particle simulations using a singular Coulomb potential is that some electrons can gain high energy and escape the cluster while others lose much energy. This unphysical process is suppressed thanks to the inclusion of recombination, which prevents the formation of tightly bound ion-electron systems.

The pulse used in our simulations has a field envelope proportional to sine squared, i.e., the laser electric field $\mathbf{F}_L$ is given by

$$\mathbf{F}_L = \mathbf{F}_0 \sin^2\frac{\pi t}{2T}\sin\omega t, \tag{9}$$

with a full width at half maximum $T$ of 100 fs and a frequency $\omega$ corresponding to a wavelength of 780 nm. $\mathbf{F}_0$ denotes the peak amplitude. The initial geometry of the clusters is chosen to be a closed-shell icosahedral structure [26] with an atom spacing of 3.7 Å for Ar and 4.4 Å for Xe [27]. The shell structure of Ar and Xe clusters is summarized in Table I.

TABLE I. Shell structure of Ar and Xe clusters. Each shell forms an icosahedron. Shells II and III contain two and three subshells, respectively.

| Shell | Subshell | Number of atoms | Distance from the center (Å) Ar | Xe |
|---|---|---|---|---|
| Central atom | | 1 | 0 | 0 |
| I | 1 | 12 | 3.7 | 4.4 |
| II | 2 | 30 | 6.3 | 7.5 |
| | 3 | 12 | 7.4 | 8.8 |
| III | 4 | 20 | 8.9 | 10.5 |
| | 5 | 60 | 9.7 | 11.4 |
| | 6 | 12 | 11.2 | 13.2 |

## III. IONIZATION MECHANISM

Figure 1 shows the temporal evolution of the mean ion charge state obtained from an $Ar_{147}$ cluster (solid line) and individual Ar atoms (dashed line) irradiated by a laser pulse with a peak intensity of $1.4\times10^{15}$ W/cm$^2$. The mean charge state obtained in a cluster gas is considerably higher than that in an atomic gas. Moreover, in our simulations highly charged ions up to $Ar^{8+}$ were obtained from the cluster gas though it is not explicitly indicated in the figure.

Our simulation method includes two possible ionization processes: tunnel (or field) ionization and electron-impact (or collisional) ionization. Strictly speaking, the distinction between tunnel ionization by an electronic field and electron-impact ionization is not unambiguous, since the latter is also due to the field of an incident electron. Nevertheless, in the present study let us refer to the ejection of a bound electron

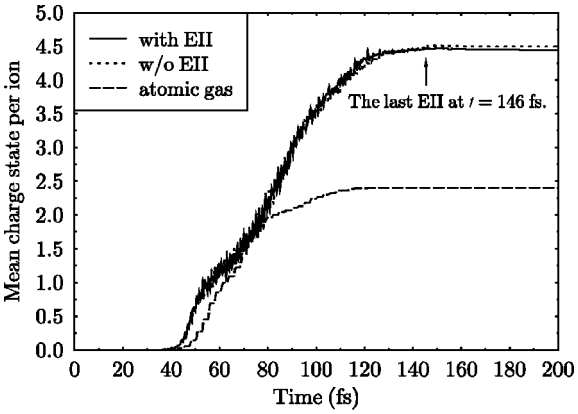


FIG. 1. Evolution of the mean charge state per ion in $Ar_{147}$ (solid line) and an atomic gas of Ar (dashed line) irradiated by the pulse with a peak intensity of $1.4\times10^{15}$ W/cm$^2$. The dotted line is the result for $Ar_{147}$ with electron-impact ionization switched off.

by an incident energetic electron as electron-impact ionization and distinguish it from tunnel ionization due to the field formed by many electrons. According to the nanoplasma model by Ditmire *et al.* [7], the principal ionization mechanism is electron-impact ionization by hot electrons. Ditmire [9] argued that this process was important even in small clusters containing only six atoms. On the other hand, the ionization ignition model by Rose-Petruck *et al.* [10] and the recent work by Last and Jortner [13] indicate that field ionization by the combined field of the laser, the other ions, and the electrons plays a dominant role, and that electron-impact ionization is of minor importance. Multiple ionization from impact by coherently moving electrons proposed in the coherent electron motion model [6] would be, if any, a purely quantum-mechanical effect, and, therefore, is outside the scope of the present study.

In order to examine the importance of electron-impact ionization on the mean charge state, we have performed a simulation with electron-impact ionization switched off, whose result is shown as a dotted line in Fig. 1. It can be seen that electron-impact ionization has practically no effect on the mean charge. We have found that this process plays only a minor role for all the cluster sizes ($Ar_{55}$, $Ar_{147}$, $Xe_{55}$, and $Xe_{147}$) we treated and for the laser intensity from $3.5\times10^{14}$ to $1.3\times10^{16}$ W/cm$^2$.

This result can be easily understood from the viewpoint of the mean free path of electrons inside the cluster. The mean free path $\lambda_{\mathrm{EII}}$ with respect to electron-impact ionization is defined by $\lambda_{\mathrm{EII}}=1/N_a\sigma_{\mathrm{EII}}(E_e)$, where $N_a$ is the atomic density inside the cluster. $\lambda_{\mathrm{EII}}$ takes the minimum value at a certain value of incident electron energy $E_e$ (minimum mean free path). We show the minimum mean free path, calculated using experimentally measured values of $\sigma_{\mathrm{EII}}$ [24,28–30], as a function of ion charge $Q$ before the ionization for Ar and Xe clusters in Fig. 2. We also indicate the diameter of the cluster containing 147 and $10^6$ atoms. As can be seen from this figure, the minimum mean free path exceeds the size of $Ar_{147}$ already at $Q=1$ and that of $Xe_{147}$ at $Q=2$. Moreover, for $Q\geqslant5$ in the case of Ar and $Q\geqslant8$ in the case of Xe, the minimum mean free path is larger than the size of a cluster containing $10^6$ atoms. It should be noted that in general the electron mean free path is larger than the minimum value plotted in Fig. 2. Hence, the contribution of electron-impact ionization is of minor importance even in the case of very large clusters. On the other hand, once several atoms are ionized, the total electric field strength at the position of each cluster ion can be significantly larger than the laser field alone. This drives further tunneling ionization and leads to high charge states just as was proposed in the ionization ignition model [10].

At a glance, our results may appear to contradict those in Ref. [9] obtained using a simulation method similar to ours. Figure 2(b) of Ref. [9] shows, however, that the level of ionization is larger when impact ionization *and* electron fields in tunnel ionization are included than when they are neglected. The effect of impact ionization *alone* was not examined in Ref. [9]. On the other hand, the present study clearly shows that electron-impact plays a negligible role in ionization, in agreement with the results in Ref. [13].

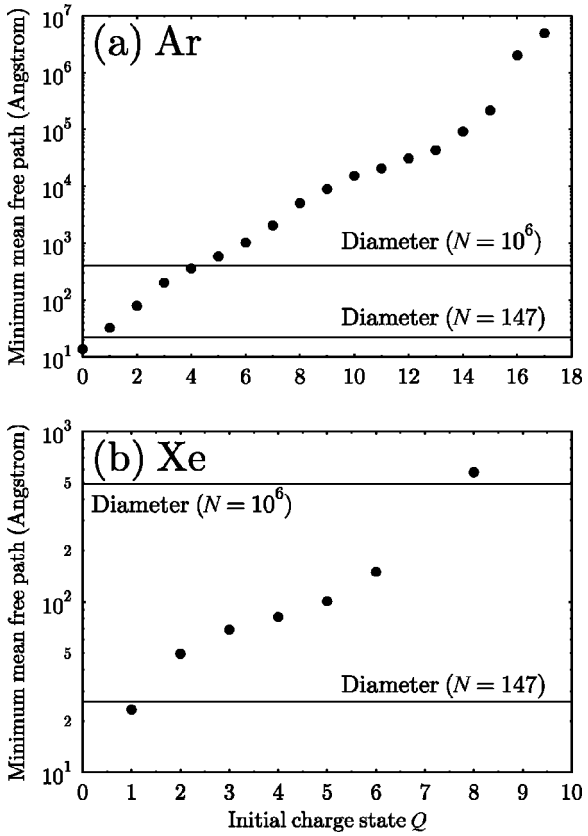


FIG. 2. (a) Minimum electron mean free path inside the Ar cluster with respect to electron-impact ionization $Ar^{Q+}\rightarrow Ar^{(Q+1)+}$ ($0\leqslant Q\leqslant17$) calculated for the incident electron energy at which the cross section $\sigma_{\mathrm{EII}}$ takes a maximum value. The diameter of an $Ar_{147}$ and $Ar_{10^6}$ is also indicated. (b) Similar plot for the case of the Xe cluster ($Q=1,\ldots,6,8$).

## IV. CHARGE DEPENDENCE OF ION ENERGY

We can consider two different explosion mechanisms of clusters irradiated by an ultrashort intense laser pulse: Coulomb explosion and hydrodynamic expansion. Coulomb explosion is expected to be a dominant mechanism in case where ejected electrons escape from the cluster quickly. In this case the accumulated total Coulomb energy is converted into ion kinetic energy. Thus, we can approximate the relation between the mean ion energy $\overline{E}=\Sigma_{j=1}^{N}E_j/N$ and the mean ion charge state $\overline{Q}=\Sigma_{j=1}^{N}Q_j/N$, with $E_j$ and $Q_j$ being the kinetic energy and the charge state, respectively, of ion $j$, and $N$ the number of atoms contained in the cluster, as

$$\overline{E}=\frac{\overline{Q}^2}{N}\sum_{i=1}^{N-1}\sum_{j=i+1}^{N}\frac{1}{|\mathbf{R}_i-\mathbf{R}_j|}\propto\overline{Q}^2, \tag{10}$$

where $\mathbf{R}_i$ denotes the initial position of ion $i$. On the other hand, one expects that the cluster explodes mainly through hydrodynamic expansion in the case where most of the free electrons are confined inside the cluster by the space-charge effect for a long time. In this case, the thermal energy of hot electrons is transformed into ion kinetic energy. Then, the

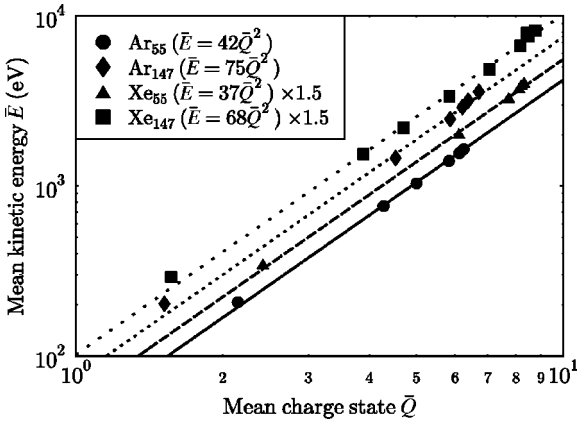


FIG. 3. Relation between the mean ion energy $\overline{E}$ and charge state $\overline{Q}$ obtained using different intensities (starting from the lowest value of $\overline{Q}$,0.35,1.4,3.2,5.6,8.8,13$\times 10^{15}$ W/cm$^2$ for $Ar_{55}$, $Ar_{147}$, and $Xe_{55}$, and 0.35, 0.79,1.0,1.4,1.9,3.2,13,5.6,8.8$\times 10^{15}$ W/cm$^2$ for $Xe_{147}$). The values of $\overline{E}$ for Xe clusters were multiplied by 1.5 for clarity.

relation between the mean energy and the mean charge of the ions is approximately given by

$$\overline{E}=\frac{3}{2}\overline{Q}k_BT_e\propto\overline{Q}, \tag{11}$$

where $k_B$ is the Boltzmann constant and $T_e$ the electron temperature. This relation is linear under the assumption that $T_e$ does not depend much on $\overline{Q}$.

Lezius *et al.* [2] obtained experimentally the charge dependence of the kinetic energy of the ions emitted from laser-irradiated Ar and Xe clusters. This dependence was used to determine when the cluster explosion is governed by the Coulomb explosion and when by hydrodynamic expansion. Their results can be summarized as follows: in the case of $Ar_N$ ($N\approx 1.8\times 10^5$) the charge dependence of the ion energy is quadratic in the entire range of $1\leqslant Q\leqslant 8$, while in the case of $Xe_N$ ($N\approx 2.0\times 10^6$), the dependence is quadratic for lower charge states ($Q<6$) and linear for higher charge states ($Q>10$). Based on these results and the discussion in the preceding paragraph, the authors of Ref. [2] have concluded that Ar clusters undergo Coulomb explosion while Xe clusters exhibit a mixed Coulomb-hydrodynamic expansion behavior. A behavior similar to the case of Xe has recently been found in the experiments with $Pb_N$ ($N\approx 300$) [14]. Hence, such a behavior appears to be a general feature which is valid over a very wide range of cluster size except for $Ar_N$. Also in Ref. [14] the quadratic dependence was attributed to the Coulomb explosion, and the linear one to hydrodynamic expansion. Equations (10) and (11) describe, however, the relation between the *mean* energy and the *mean* charge state of the ions, and do not necessarily hold true for the charge-energy relation of *individual* ions, obtained in these experiments [2,14]. In what follows, we examine the charge-energy relation obtained from our simulation results in detail.

In Fig. 3 we plot the relation between the mean ion energy

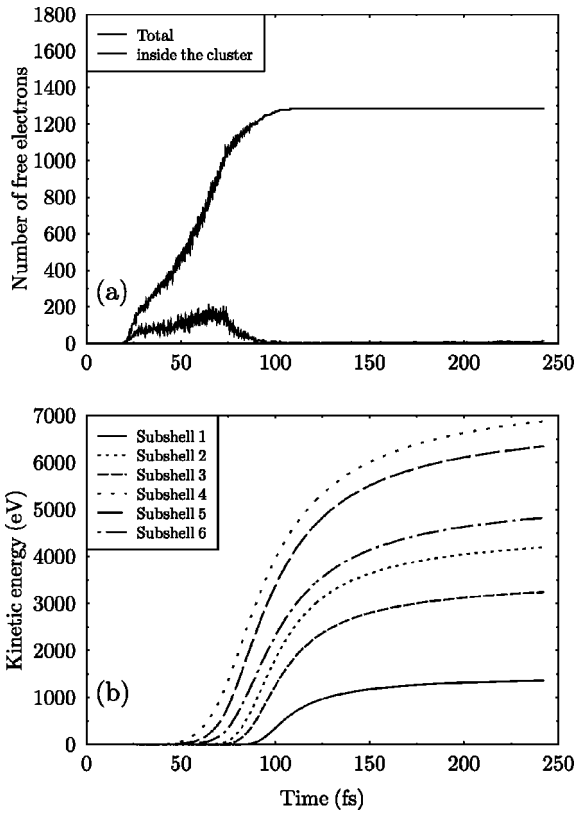


FIG. 4. (a) Evolution of the total number of free electrons (upper line) and the number of free electrons whose distance from the origin (the initial position of the central atom) is smaller than that of the outermost ion (lower line) for the case of a $Xe_{147}$ cluster irradiated by the pulse with a peak intensity of $8.8\times 10^{15}$ W/cm$^2$. (b) Evolution of the mean ion energy of each subshell, for the case of (a).

$\overline{E}$ and mean charge state $\overline{Q}$ obtained using different laser intensities for $Ar_{55}$, $Ar_{147}$, $Xe_{55}$, and $Xe_{147}$. The relation can be modeled with $\overline{E}\approx\alpha\overline{Q}^2$, where $\alpha$ is a constant. This indicates that ions are accelerated mainly through a Coulomb explosion mechanism. The value of $\alpha$ indicated in Fig. 3 is smaller than the one (57, 115, 41, and 75 eV for $Ar_{55}$, $Ar_{147}$, $Xe_{55}$, and $Xe_{147}$, respectively) which can be calculated from Eq. (10). This is because the charge state of each ion changes in time, and because the cluster explosion begins before the ion charges reach their final values.

In Fig. 4(a) we show the temporal evolution of the total number of free electrons and the number of free electrons inside the cluster for the case of a $Xe_{147}$ cluster irradiated by a laser pulse with a peak intensity of $8.8\times 10^{15}$ W/cm$^2$. Figure 4(b) shows the evolution of the mean kinetic energy of ions from each subshell. From these figures we can see that electrons quit the cluster before the main stage of ion acceleration without exchanging significant energy with ions. This excludes a hydrodynamic scenario and indicates that the ions are accelerated mainly by their mutual Coulomb repulsion. Figure 4(b) also shows a stepwise character of the cluster explosion. The explosion is neither instantaneous nor uniform: the ions are accelerated in sequence from outer shells, and those leaving first are more energetic than those leaving

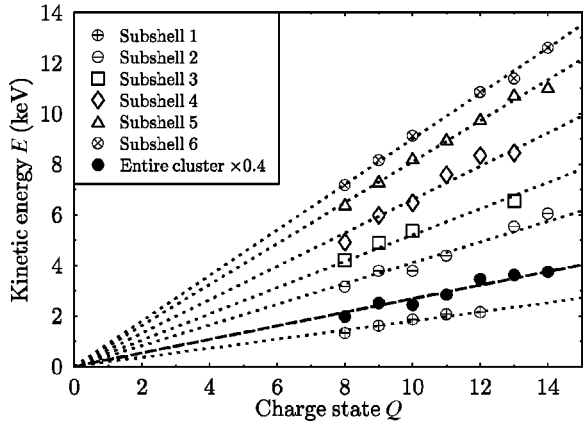


FIG. 5. Mean ion kinetic energy $E(Q)$ as a function of charge state $Q$ for each subshell of $Xe_{147}$ and for the entire cluster (filled circles, multiplied by 0.4 for clarity) in the case of a peak intensity $8.8\times10^{15}$ W/cm$^2$. The subshells are enumerated outwards starting from the innermost one.

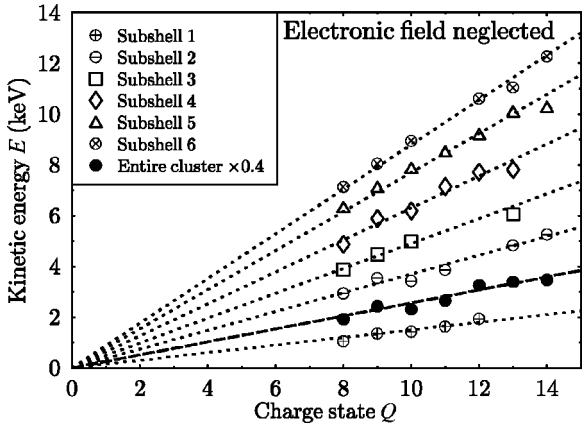


FIG. 6. Mean ion kinetic energy $E(Q)$ as a function of charge state $Q$ for each subshell of $Xe_{147}$ and for the entire cluster (filled circles, multiplied by 0.4 for clarity), obtained by neglecting the electronic field term in the ionic equation of motion for the case of Fig. 5.

later. This feature, also observed in one-dimensional Thomas-Fermi simulations [31] and in smoothed particle hydrodynamics simulations [32], can be understood on the basis of the ionization ignition mechanism [10] and Coulomb explosion. Seen by an ion in outer shells, the fields from the other ions add up to a large value while seen by an ion in inner shells, they cancel each other partly. Thus the ions in outer shells are ionized earlier and, at the same time, more effectively accelerated than those in inner shells.

Let us now turn to the charge-energy relation of individual ions. Rare-gas clusters have a shell structure as is shown in Table I. We consider the charge and energy distribution of ions originating from each subshell. We denote the mean kinetic energy of the ions with a charge of $Q$, originating from subshell $s$ as $E_s(Q)$. It should be noted that neither $E_s(Q)$ nor its average over all the cluster subshells is identical to $\overline{E}$, plotted in Fig. 3. The latter is the mean energy of all the cluster ions, regardless of their charge state $Q$. On the other hand, for a given value of $Q$, $E_s(Q)$ involves only the ions with this charge state. $\overline{E}$ can be written in terms of $E_s(Q)$ as

$$\overline{E}=\frac{1}{N}\sum_s N_s\sum_Q Y_s(Q)E_s(Q), \tag{12}$$

where $N_s$ is the number of the ions contained in subshell $s$, satisfying $N=\Sigma_s N_s$, while $Y_s(Q)$ is the probability distribution of $Q$ in subshell $s$, normalized as $\Sigma_Q Y_s(Q)=1$. Using $Y_s(Q)$, the mean charge state $\overline{Q}$ can be written as

$$\overline{Q}=\frac{1}{N}\sum_s N_s\sum_Q Y_s(Q)Q. \tag{13}$$

In Fig. 5 we plot $E_s(Q)$ as a function of charge state $Q$ for each subshell $s(s=1,\ldots,6)$ of $Xe_{147}$ in the case of a peak intensity $8.8\times10^{15}$ W/cm$^2$. We can model the relation in Fig. 5 with $E_s(Q)\approx\beta_s Q$, where a constant $\beta_s$ depends on $s$. It should be emphasized that the approximately linear dependence in Fig. 5 is a consequence of the Coulomb explosion, which dominates the cluster explosion in our simulation results. This behavior can be understood as follows. Let us consider a pure Coulomb explosion of clusters composed of $N$ ions with charges $Q_i(i=1,\ldots,N)$ randomly chosen according to the probability distribution $Y_s(Q_i)$ depending on $s$. In general, the final kinetic energy $E_1$ of an ion with a charge $Q_1$ in subshell $s_1$ is a complicated function of $Q_1,\ldots,Q_N$. In order to estimate the average $\hat{E}_1$ of $E_1$ over the distribution of $Q_2,\ldots,Q_N$, we may assume that the cluster expands in average nearly isotropically and that the effect of the other ions in subshell $s_1$ is negligible. Then $\hat{E}_1$ can be roughly written as

$$\hat{E}_1(Q_1)\approx\frac{Q_1\Sigma_{i\in s<s_1}\overline{Q_i}}{r_1}\propto Q_1, \tag{14}$$

where the sum is taken over all the ions in inner subshells and at the center, $r_1$ denotes the initial distance of the ion from the central ion, and $\overline{Q_i}\equiv\Sigma_{Q_i}Y_s(Q_i)Q_i$ is the expectation value of $Q_i$. The value of $\beta_s$ is different from $\Sigma_{i\in s<s_1}\overline{Q_i}/r_1$ in general, since in simulations $Q_i$ depends on time, there is screening of ion charges by free electrons, and the effect of the others ions in the same subshell is not completely negligible.

We simulated the Coulomb explosion of $Xe_{147}$ by dropping the electronic field term in the ionic equations of motion but taking account of the ion charge history obtained for the case of Fig. 5. The resulting charge-energy relation, shown in Fig. 6, is very similar to that in Fig. 5, except that the obtained ion energy is slightly smaller, whose mechanism will be discussed in Sec. V. This confirms that the contribution of the electronic field to the acceleration of the ions is very small and that the linear relation is due to Coulomb explosion. If $Y_s(Q)$ is independent of $s$, the average $E(Q)$ of $E_s(Q)$ over the entire cluster is also proportional to $Q$. In Fig. 5 we have plotted $E(Q)$ as filled circles. We see a linear

relation except for small deviation due to the dependence of $Y_s(Q)$ on $s$. We have found that this holds approximately also for $Ar_{55}$, $Ar_{147}$, and $Xe_{55}$ and for other values of laser intensity. The preceding discussion has an important impact on the interpretation of the experimental results by Lezius *et al.* [2] and Viallon [14]. These authors attributed the linear dependence at higher charge states observed in their experiments to hydrodynamic expansion. Our results, however, indicate that this interpretation is not necessarily correct.

As we have already mentioned, Lezius *et al.* [2] and Viallon [14] found a quadratic charge dependence of ion energy for lower charge states and a linear dependence for higher charge states. We observe such a behavior in our simulation results (see below). In order to understand it, we have to take into account that the laser intensity has a spatial profile in experimental situations. Let us denote the mean energy and the relative yield of ions with a charge $Q$ from clusters irradiated by a laser pulse with a peak intensity $I$ by $E(I,Q)$ and $Y(I,Q)$, respectively. As we have seen in Fig. 5, $E(I,Q)$ can be roughly modeled with

$$E(I,Q)=\beta(I)Q, \tag{15}$$

where $\beta(I)$ is a coefficient depending on $I$. On the other hand, we can model the relation between

$$\overline{E}(I)\equiv\sum_Q Y(I,Q)E(I,Q) \tag{16}$$

and

$$\overline{Q}(I)\equiv\sum_Q Y(I,Q)Q, \tag{17}$$

with

$$\overline{E}(I)=\alpha\overline{Q}(I)^2, \tag{18}$$

as we have seen in Fig. 3. It follows from Eqs. (15) and (18) along with Eqs. (16) and (17) that

$$\beta(I)=\alpha\overline{Q}(I). \tag{19}$$

We can write the average $\langle E\rangle(Q)$ of $E(I,Q)$ over the spatial intensity profile, which corresponds to the charge-energy relation observed in experiments, as

$$\langle E\rangle(Q)=\frac{\alpha Q\int w(I)Y(I,Q)\overline{Q}(I)dI}{\int w(I)Y(I,Q)dI}, \tag{20}$$

where we have used Eqs. (15) and (19), and $w(I)$ is a weighting function, determined by the laser profile. The mean charge state $\overline{Q}(I)$ is a function of intensity $I$ and, in general, it takes a maximum at $I=I_{\max}$, where $I_{\max}$ is the maximum peak intensity. It should be noted that $\overline{Q}(I_{\max})$ is the maximum value of the mean charge state, *not* the highest charge state obtained. In fact, some ions have a charge much greater than $\overline{Q}(I_{\max})$. We can divide the whole range of $Q$ into two parts: $Q<\overline{Q}(I_{\max})$ and $Q>\overline{Q}(I_{\max})$.

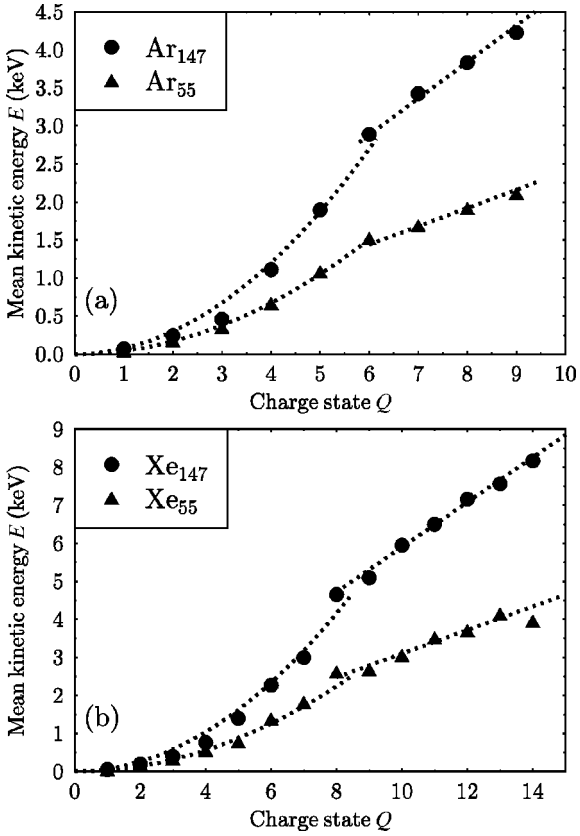


FIG. 7. Charge dependence of ion energy of (a) $Ar_{55}$, $Ar_{147}$ and (b) $Xe_{55}$, $Xe_{147}$ irradiated by the laser pulse with a peak intensity of $1.3\times10^{16}$ W/cm$^2$ with an account of the spatial intensity profile.

In the case where $Q<\overline{Q}(I_{\max})$, the main contribution comes from such an intensity range that satisfies $\overline{Q}(I)\approx Q$, since $Y(I,Q)$ peaks at the value of $Q$ around $\overline{Q}(I)$. Hence we may replace $\overline{Q}(I)$ in Eq. (20) by $Q$ and obtain

$$\langle E\rangle(Q)\approx\alpha Q^2\propto Q^2 \quad \text{if} \quad Q<\overline{Q}(I_{\max}). \tag{21}$$

On the other hand, for all the values of $Q$ which satisfy $Q>\overline{Q}(I_{\max})$, the most important contribution comes from the same spatial region of such high intensity that $\overline{Q}(I)\approx\overline{Q}(I_{\max})$, since a significant portion of atoms are ionized to high charge states only there. Then, replacing $\overline{Q}(I)$ in Eq. (20) by $\overline{Q}(I_{\max})$, we obtain

$$\langle E\rangle(Q)\approx\beta(I_{\max})Q\propto Q \qquad \text{if} \quad Q>\overline{Q}(I_{\max}). \tag{22}$$

In short, the behavior for $Q<\overline{Q}(I_{\max})$, which reflects Eq. (18), contains the contribution from the entire intensity range, while that for $Q>\overline{Q}(I_{\max})$ contains the contribution only from the intensity range close to $I_{\max}$.

Figure 7 illustrates the ion energy-charge relation we obtained by taking average over the simulation results for $Ar_{55}$, $Ar_{147}$, $Xe_{55}$, and $Xe_{147}$ with different values of intensity as

in Fig. 3. The average was taken with an equal weight, since our discussion in the previous paragraph does not depend much on the form of $w(I)$. As expected, for each of the four cases the dependence of ion energy $\langle E \rangle$ on $Q$ is approximately quadratic for lower charge states $Q \leqslant Q_c$ ($Q_c = 6$ for Ar, 8 for Xe) and is linear for higher charge states $Q \geqslant Q_c$. These values of $Q_c$ agree well with those of $\overline{Q}(I_{\max})$, i.e., the highest value of the mean charge state that we can obtain from Fig. 3. It should be emphasized again that the charge-energy relation in Fig. 7 is a consequence of Coulomb explosion.

In Ref. [2] the relation was reported to be quadratic in the entire range of $1 \leqslant Q \leqslant 8$ in the case of Ar. This may be explained as follows. The laser intensity needed to obtain $Ar^{8+}$ and $Ar^{9+}$ via tunnel ionization is $2.6 \times 10^{16}$ W/cm$^2$ and $1.6 \times 10^{18}$ W/cm$^2$, respectively. The large difference between these two values is due to the fact that the ionization potential of $Ar^{8+}$ (422 eV [33]) is much higher than that of $Ar^{7+}$ (143 eV [33]). The peak intensity ($5 \times 10^{17}$ W/cm$^2$) used in Ref. [2] was sufficient to obtain a significant number of $Ar^{8+}$, but too low to ionize Ar nine times even with the aid of the ionization ignition mechanism. Since this corresponds to $\overline{Q}(I_{\max}) = 8$, a quadratic charge-energy relation was observed for $1 \leqslant Q \leqslant 8$. On the other hand, the yield of $Ar^{Q+}$ ($Q \geqslant 9$), for which a linear dependence should be expected, was very low.

## V. ANGULAR DEPENDENCE OF ION ENERGY

In the present section we examine the ion acceleration mechanism in some more detail. Figure 8(a) shows the ion energy as a function of angle with respect to the direction of laser polarization. This figure indicates that the cluster explosion is not completely isotropic: the energy of ions is higher when they are emitted along the direction of laser polarization rather than perpendicular to it. This observation becomes more evident if we draw a similar plot only for ions with a final charge state $Q$ equal to 8 as in Fig. 8(b). Such a trend was also observed in recent experiments by Springate *et al.* [8]. The field acting on each ion is composed of three contributions: ionic, electronic, and laser fields. The ionic field alone, which plays the most important role of these three in the acceleration of ions, cannot explain the trend found in Fig. 8. This can be seen if we compare Fig. 8(b) with Fig. 9, in which we have plotted the angular dependence of the energy of the ions with $Q = 8$ obtained by dropping the electronic and laser field terms in the equation of motion of each ion (i.e., the ions are accelerated exclusively by their mutual Coulomb repulsion) but taking account of the charge history of each ion for the case of Fig. 8. In order to investigate the impact of the contributions from the laser field, we have also performed simulations in which we neglect only the electronic field term in the ionic equation of motion. The resulting angular dependence of the energy of the ions with $Q = 8$ is shown in Fig. 10. The effect of the laser field is obtained as the difference of Figs. 10 and 9, and is plotted in Fig. 11(a). Similarly, the effect of the electric field is obtained as the difference of Figs. 8(b) and 10, and is plotted in 11(b). We can clearly see that it is the effect of the laser field that leads to the anisotropy.

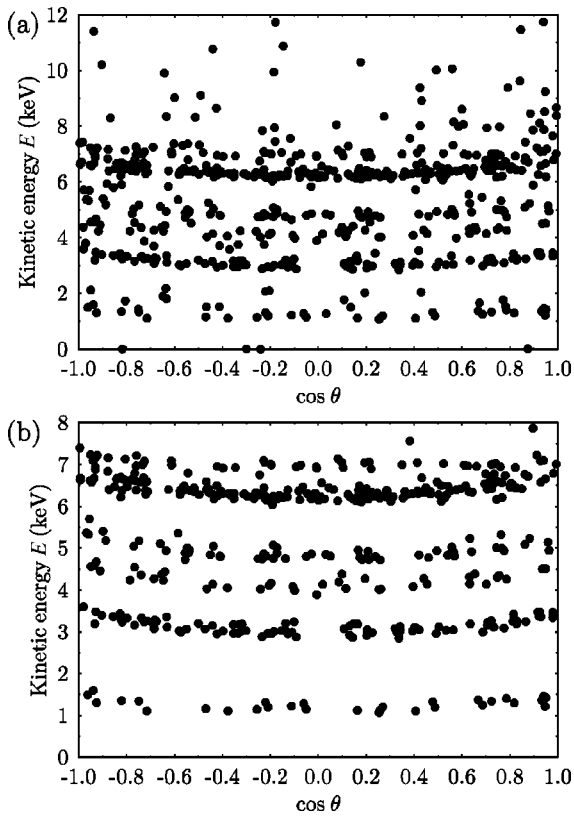


FIG. 8. (a) Dependence of the kinetic energy on the cosine of the angle $\theta$ between the laser polarization vector and the emitted direction of the ions for the case of $Xe_{147}$ irradiated by the laser pulse with a peak intensity of $8.8 \times 10^{15}$ W/cm$^2$. Each filled circle corresponds to an ion obtained from four simulations. (b) Similar plot only for the ions with a charge state of 8.

Let us consider how the laser field contributes to the acceleration of a cluster ion ejected in the direction of the laser polarization vector. Seen by this ion, the laser field points to the outward direction during the first half optical cycle and to the inward direction during the second half, contributing al-

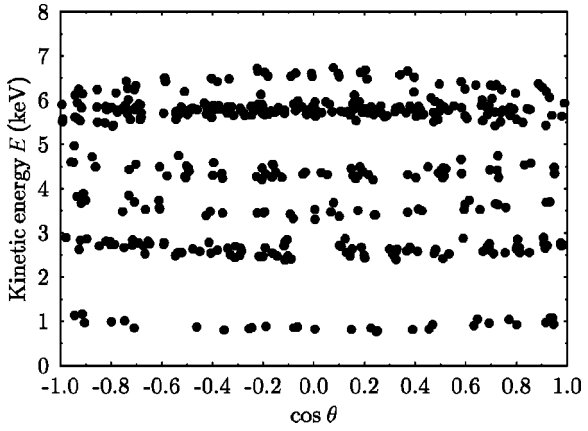


FIG. 9. Similar to Fig. 8(b) for the case of the simulations in which only the field from the other ions is taken into account in the equation of motion of each ion.

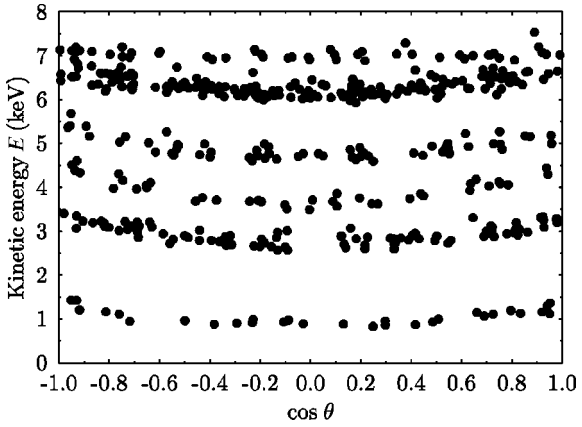


FIG. 10. Similar to Fig. 8(b) for the case of the simulations in which only the fields from the other ions and the laser are taken into account in the equation of motion of each ion.

ternatingly to acceleration and deceleration. Thus, its net effect would be negligible if the ion charge were a constant throughout the optical cycle. The ion charge, however, depends on time. In Fig. 12 we show typical charge histories for the case where an ion is ejected along the direction of laser polarization and perpendicular to it. When the ion is emitted along the laser polarization (dashed line), its charge state changes significantly even within one optical cycle. It should be noted that the sum of the fields from the other ions and the electrons points to the outward direction all the time. During the first half cycle the laser field adds to these fields, and a higher charge state is reached via tunnel ionization by the total field. This leads to an efficient ion acceleration. During the second half cycle, on the other hand, the laser field is antiparallel to the field from the other particles. The total field is not sufficient to maintain a high charge state, and the recombination with electrons leads to a lower charge state. Thus the ion deceleration during the second half cycle is not so efficient as the acceleration during the first, which results in a net acceleration within one entire optical cycle. Such an effect is less prominent for ions ejected in the direction perpendicular to the laser polarization, since their charge remains nearly constant within one optical cycle in most cases as can be seen in Fig. 12 (solid line).

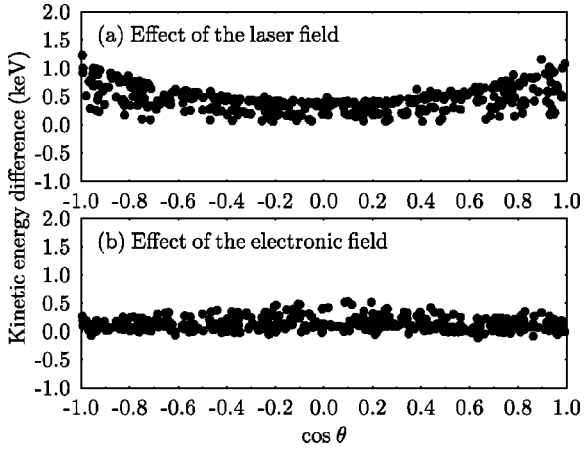


FIG. 11. The difference of the ion energy (a) between Figs. 10 and 9 and (b) between Figs. 8(b) and 10 as a function of the value of cos$\theta$ obtained for the case of Fig. 8(b).

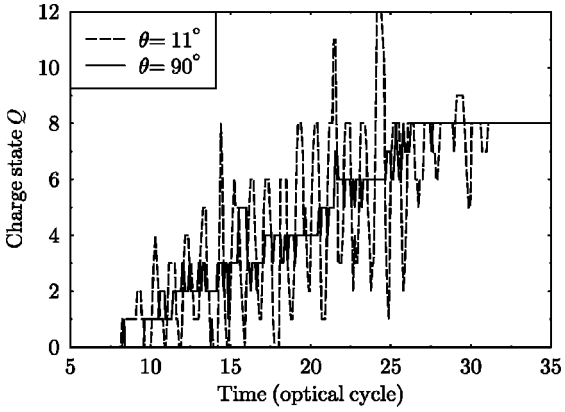


FIG. 12. Examples of the charge history of the ions ejected from subshell 5 of $Xe_{147}$ for the case of Fig. 8 in the direction nearly parallel ($\theta = 11°$, dashed line) and perpendicular ($\theta = 90°$, solid line) to the laser polarization.

Our simple implementation of ion-electron recombination may not reproduce its rate very accurately. Moreover, a discrete, integer-valued ''charge state'' cannot be rigorously defined in situations where many electrons may reside near the ion and where ionization and recombination may often take place, since there exists no quantum-mechanical operator corresponding to this quantity. Nevertheless, we believe that the above explanation is still valid in real situations, translating into the following one: the electron cloud, including free electrons, is significantly less localized near the nucleus during the first half optical cycle than in the second half, and this leads to a net laser-field-induced acceleration of the ions emitted along the direction of laser polarization.

From Fig. 11(b) we can see that the ions are accelerated to slightly higher energy in the simulation including the electronic field term in the ionic equation of motion than in the simulation neglecting it. A similar trend can be found if we compare Figs. 5 and 6. This is, paradoxally, due to the screening of the ion charge by free electrons. At an early stage of the cluster explosion, where a portion of free electrons reside inside the cluster, the ion is less efficiently accelerated because of the screening when the field from electrons are included in the simulation. As a consequence, when the ion charge has reached its final value and most of free electrons have escaped the cluster, the ions are still closely packed together, and more Coulomb energy is accumulated than when the electronic field is neglected in the ionic equation of motion. This results in higher final ion kinetic energy.

## VI. CONCLUSIONS

We have studied the explosion of rare-gas clusters containing up to 147 atoms in an intense laser field using Monte Carlo classical particle-dynamics simulations. The ionization ignition mechanism [10] dominates cluster ionization, while the electron-impact ionization plays only a minor role. This follows from the fact that the electron mean free path with

respect to this process is typically larger than the cluster size.

Although the cluster size treated in the present study is relatively small, our detailed analysis of ion kinetic energy has provided several interesting findings. The cluster ions are accelerated mainly by the Coulomb repulsion force between themselves. Free-electrons escape from the cluster without exchanging significant energy with ions, and hardly contribute to the cluster explosion except screening of the ion charges at an early stage of the explosion. Even though these observations may not be surprising for the cluster size in the present study, this Coulomb explosion leads to the qualitatively same charge dependence of ion kinetic energy as that found in experiments [2,14] with larger clusters. Especially, we have found a linear dependence at higher charge states, which was formerly attributed to hydrodynamic expansion. We have shown that the entire charge-energy relation can be understood as a consequence of Coulomb explosion and the effect of the spatial laser intensity variation. Our finding can affect the interpretation of experimental results.

Nevertheless, unlike a pure Coulomb explosion, the cluster explosion is neither uniform nor isotropic. Our results show that cluster ions are accelerated in sequence from outer shells and that the energy of ions is higher when they are emitted along the direction of laser polarization than perpendicular to it. The charge state of the ions emitted in the direction parallel to laser polarization changes in resonance with the laser field, and this leads to the net acceleration of ions, which is absent in the direction perpendicular to laser polarization.

## ACKNOWLEDGMENTS

We would like to thank M. Schmidt, C. Ellert, J. Viallon, and M.-A. Lebeault for fruitful discussions.

## APPENDIX: KUSTAANHEIMO-STIEFEL (KS) REGULARIZATION

In this appendix we briefly summarize the Kustaanheimo-Stiefel regularization [19–21]. The equations of the perturbed relative two-body (ion-electron) motion have the form

$$\frac{d^2\mathbf{r}}{dt^2}+\frac{Q}{mr^3}\mathbf{r}=\frac{\partial V}{\partial \mathbf{r}}+\mathbf{F}, \tag{A1}$$

where $\mathbf{r}=(r_1,r_2,r_3)$ denotes the relative position vector, $r=|\mathbf{r}|$, and $m$ the reduced mass. The ''ion charge'' $Q$ may depend on $r$. The right-hand side describes the force from a disturbing potential $V$ and a nonpotential disturbing force $\mathbf{F}$. The KS variables are the components of the four-dimensional vector $\mathbf{u}=(u_1,u_2,u_3,u_4)$ of the parametric space related to the three-dimensional vector $\mathbf{r}$ of the physical space by the KS transformation,

$$\mathbf{r}=L(\mathbf{u})\mathbf{u}, \tag{A2}$$

with

$$L(\mathbf{u})=\begin{pmatrix} u_1 & -u_2 & -u_3 & u_4 \\ u_2 & u_1 & -u_4 & -u_3 \\ u_3 & u_4 & u_1 & u_2 \end{pmatrix}. \tag{A3}$$

It follows from Eq. (A2) that

$$r=|\mathbf{r}|=|\mathbf{u}|^2. \tag{A4}$$

The initial transformation from $\mathbf{r}$ into $\mathbf{u}$ is achieved [20] by

$$u_1=\sqrt{(r+r_1)/2},\quad u_2=r_2/2u_1,\quad u_3=r_3/2u_1,\quad u_4=0, \tag{A5}$$

if $r_1>0$, and by

$$u_2=\sqrt{(r-r_1)/2},\quad u_1=r_2/2u_2,\quad u_3=0,\quad u_4=r_3/2u_2, \tag{A6}$$

if $r_1\leqslant 0$. If we introduce the fictitious time $s$ obeying the relation,

$$\frac{dt}{ds}=r, \tag{A7}$$

we obtain

$$\frac{d\mathbf{r}}{dt}=\frac{2}{r}L(\mathbf{u})\frac{d\mathbf{u}}{ds}\qquad\text{and}\qquad\frac{d\mathbf{u}}{ds}=\frac{1}{2}L^T(\mathbf{u})\frac{d\mathbf{r}}{dt}, \tag{A8}$$

where $L^T$ denotes the transposed matrix of $L$. We also obtain

$$L^T(\mathbf{u})\frac{\partial V}{\partial \mathbf{r}}=\frac{1}{2}\frac{\partial V}{\partial \mathbf{u}}. \tag{A9}$$

Then we can rewrite the equation of motion Eq. (A1) as

$$\frac{d^2\mathbf{u}}{ds^2}+\frac{1}{2}h_K\mathbf{u}=\frac{1}{2}|\mathbf{u}|^2\left(\frac{1}{2}\frac{\partial V}{\partial \mathbf{u}}+L^T(\mathbf{u})\mathbf{F}\right), \tag{A10}$$

with

$$h_K=\frac{Q}{mr}-\frac{2}{r}\left|\frac{d\mathbf{u}}{ds}\right|^2=\frac{Q}{mr}-\frac{1}{2}\left|\frac{d\mathbf{r}}{dt}\right|^2, \tag{A11}$$

which is the binding energy of the Keplerian motion divided by $m$ if $Q$ is constant. This equation involves the equation for $r$,

$$\frac{d^2r}{ds^2}+2h_Kr=\frac{Q}{m}+r\left(\frac{\partial V}{\partial \mathbf{r}}+\mathbf{F}\right)\cdot\mathbf{r}. \tag{A12}$$

Since Eq. (A10) has the same form as the equation of motion for a perturbed harmonic oscillator, it is much easier to handle numerically than Eq. (A1) when $r$ is very small.

[1] M. Lezius, S. Dobosz, D. Normand, and M. Schmidt, J. Phys. B **30**, L251 (1997).
[2] M. Lezius, S. Dobosz, D. Normand, and M. Schmidt, Phys. Rev. Lett. **80**, 261 (1998).
[3] T. Ditmire, J.W.G. Tisch, E. Springate, M.B. Mason, N. Hay, R.A. Smith, J. Marangos, and M.H.R. Hutchinson, Nature (London) **386**, 54 (1997).
[4] Y.L. Shao, T. Ditmire, J.W.G. Tisch, E. Springate, J.P. Marangos, and M.H.R. Hutchinson, Phys. Rev. Lett. **77**, 3343 (1996).
[5] B.D. Thompson, A. McPherson, K. Boyer, and C.K. Rhodes, J. Phys. B **27**, 4391 (1994).
[6] K. Boyer, B.D. Thompson, A. McPherson, and C.K. Rhodes, J. Phys. B **27**, 4373 (1994).
[7] T. Ditmire, T. Donnelly, A.M. Rubenchik, R.W. Falcone, and M.D. Perry, Phys. Rev. A **53**, 3379 (1996).
[8] E. Springate, N. Hay, J.W.G. Tisch, M.B. Mason, T. Ditmire, M.H.R. Hutchinson, and J.P. Marangos, Phys. Rev. A **61**, 063201 (2000).
[9] T. Ditmire, Phys. Rev. A **57**, R4094 (1998).
[10] C. Rose-Petruck, K.J. Schafer, K.R. Wilson, and C.P.J. Barty, Phys. Rev. A **55**, 1182 (1997).
[11] I. Last and J. Jortner, J. Phys. Chem. A **102**, 9655 (1998).
[12] I. Last and J. Jortner, Phys. Rev. A **60**, 2215 (1999).
[13] I. Last and J. Jortner, Phys. Rev. A **62**, 013201 (2000).
[14] J. Viallon, Ph.D. thesis, Université de Lyon, Lyon, France, 2000.
[15] P.B. Corkum, N.H. Burnett, and F. Brunel, Phys. Rev. Lett. **62**, 1259 (1989).
[16] P.B. Corkum, Phys. Rev. Lett. **71**, 1994 (1993).
[17] E. Clementi and D.L. Raimondi, J. Chem. Phys. **38**, 2686 (1963).
[18] W. H. Press, S. A. Teukolsky, W. T.Vetterling, and B. P. Flannery, *Numerical Recipes in FORTRAN* (Cambridge University Press, Cambridge, 1992).
[19] P. Kustaanheimo and E. Stiefel, J. Reine Angew. Math. **218**, 204 (1965).
[20] S.J. Aarseth, in *Multiple Time Scales*, edited by J.U. Brackbill and B.I. Cohen (Academic Press, Orlando, 1985), p. 377.
[21] V.A. Brumberg, *Analytical Techniques of Celestial Mechanics* (Springer-Verlag, Berlin, 1995).
[22] A.M. Perelomov, V.S. Popov, and M.V. Terent'ev, Zh. Éksp. Teor. Fiz. **50**, 1393 (1966) [Sov. Phys. JETP **23**, 924 (1966)].
[23] M.V. Ammosov, N.B. Delone, and V.P. Kraĭnov, Zh. Éksp. Teor. Fiz. **91**, 2008 (1986) [Sov. Phys. JETP **64**, 1191 (1986)].
[24] M.A. Lennon, K.L. Bell, H.B. Gilbody, J.G. Hughes, A.E. Kingston, M.J. Murray, and F.J. Smith, J. Phys. Chem. Ref. Data **17**, 1285 (1988).
[25] W. Lotz, Z. Phys. **216**, 241 (1968).
[26] J.A. Northby, J. Chem. Phys. **87**, 6166 (1987).
[27] A. Bondi, J. Phys. Chem. **68**, 441 (1964).
[28] E.W. Bell, M. Djurić, and G.H. Dunn, Phys. Rev. A **48**, 4286 (1993).
[29] D.C. Griffin, C. Bottcher, M.S. Pindzola, S.M. Younger, D.C. Gregory, and D.H. Crandall, Phys. Rev. A **29**, 1729 (1984).
[30] M.E. Bannister, D.W. Mueller, L.J. Wang, M.S. Pindzola, D.C. Griffin, and D.C. Gregory, Phys. Rev. A **38**, 38 (1988).
[31] M. Brewczyk and K. Rzążewski, Phys. Rev. A **60**, 2285 (1999).
[32] M. Rusek, H. Lagadec, and T. Blenski, Phys. Rev. A (to be published).
[33] R. D. Cowan, *the Theory of Atomic Structure and Spectra* (University of California Press, Berkeley, 1981), p. 12.